Heliyon 10 (2024) e37258

Contents lists available at ScienceDirect

Heliyon

journal homepage: www.cell.com/heliyon

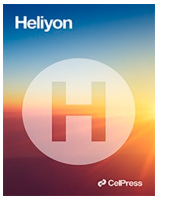

Research article

Novel homozygous missense variants in *MED27* associated with neurodevelopmental disorder: Clinical and pathogenetic research

Gongao Wu, Ruofei Lian, Mengchun Li, Liang Jin, Tianming Jia, Lijun Wang, Ling Gan, Shichao Zhao, Ruirui Liang, Yan Dong *

Department of Pediatrics, The Third Affiliated Hospital of Zhengzhou University, Zhengzhou, Henan Province, China

ARTICLE INFO

Keywords:
MED27 gene variant
NEDSCAC
Global developmental delay
Genetics

ABSTRACT

Background: Neurodevelopmental disorder with spasticity, cataracts, and cerebellar hypoplasia (NEDSCAC), induced by *MED27* gene, is an autosomal recessive rare disorder characterized by widespread developmental delay with varying degrees of intellectual impairment. Other symptoms include limb spasticity, cataracts, and cerebellar hypoplasia. So far there have been limited reports on NEDSCAC.

Methods: In this study, we conducted genetic testing on a child presenting with developmental delay as the primary clinical feature. The genetic test results indicated the presence of novel homozygous missense variants c.74G > A, p.(Arg25His) in the *MED27* gene. *In vitro* functional validation experiments, including plasmid construction and cell transfection, Western blotting, and molecular dynamics structural modeling, were performed on the MED27 Arg25His variant.

Results: The results demonstrated a significant reduction in protein expression of MED27 Arg25His and indicated may weaken the interaction force between the MED27 subunit and MED14 subunit.

Conclusions: This study expands our understanding of *MED27* gene variants and their associated clinical phenotypes. Additionally, it contributes to the investigation of the potential pathogenesis of NEDSCAC caused by *MED27* gene variants.

1. Introduction

Neurodevelopmental disorder with spasticity, cataracts, and cerebellar hypoplasia (NEDSCAC) is a recently identified autosomal recessive disorder (OMIM: 619286)-a rarely reported disease up to now. Furthermore, research on the pathogenesis of this disease is quite limited. In this report, we presented a case of a child diagnosed with NEDSCAC through whole-exome sequencing (WES), which revealed a novel missense variant at c.74G > A, p.(Arg25His). This is the first time reported in China. This discovery in the *MED27* gene expands the clinical and genetic spectrum associated with NEDSCAC, adding to our understanding of this emerging neurodevelopmental condition.

Global developmental delay, intellectual impairment, central hypotonia, limb stiffness, dystonia, and, in severe cases, cataracts and seizures are the features of NEDSCAC [1,2]. Brain imaging typically reveals cerebellar hypoplasia along with other abnormalities such

* Corresponding author.
E-mail addresses: w1354677939@163.com (G. Wu), rrxtc990712@126.com (R. Lian), limengchun2018@163.com (M. Li), jinliang0212@126.com (L. Jin), jtm226@sina.com (T. Jia), wang1022lijun@163.com (L. Wang), ganling512@163.com (L. Gan), zhaoscyh@163.com (S. Zhao), 1528719785@qq.com (R. Liang), yjs6690@126.com (Y. Dong).

https://doi.org/10.1016/j.heliyon.2024.e37258
Received 22 February 2024; Received in revised form 4 August 2024; Accepted 29 August 2024
Available online 3 September 2024

as cerebral shrinkage, myelosclerosis, and a thin corpus callosum. In 2021, Meng et al. reported on 16 patients from 11 families who had variants in both alleles of the *MED27* gene. They summarized the clinical phenotypes and morphological manifestations and conducted an initial exploration of the correlation between genotypes and phenotypes, proposing the concept of NEDSCAC. Continuing this research, Maroofian et al., in 2023 compiled the genotypes, clinical phenotypes, and neuroimaging manifestations of previously reported cases as well as new patients. They conducted an in-depth investigation into the genotype-phenotype correlation and neuroimaging findings, establishing the concept of "Neuro-MEDopathies". Furthermore, they suggested considering differential diagnoses with syndromes of cerebello-lental neurodegeneration and other subtypes of "Neuro-MEDopathies".

The *MED27* gene encodes the MED subunit 27, which belongs to the MED complex family [3]. The Mediator multiprotein complex (MED) is responsible for controlling the transcription of almost all RNA polymerase II-dependent genes, exhibiting high evolutionary conservation among eukaryotes [3]. Additionally, MED plays a significant role in chromatin remodeling, epigenetic regulation, and the processing of mRNA and non-coding RNA, contributing to various aspects of transcriptional regulation [4]. Dysfunction or abnormal expression of Mediator has been linked to developmental diseases and cancer, emphasizing its critical role in multicellular organism development [4–8].

2. Material and method

2.1. Patient and ethical statement

This study focused on a male child who received diagnosis and monitoring at the Pediatric Neurology Department of the Third Affiliated Hospital of Zhengzhou University. Genetic testing revealed the presence of homozygous missense variants c.74G > A, p.(Arg25His) in the *MED27* gene, which was identified at the age of 7 months. Informed consent was obtained from the parents of the patient, and ethical statements were obtained from Medical Ethics Committee of The Third Affiliated Hospital of Zhengzhou University (Reference: 2023-(Pre)202). All the procedures were performed in accordance with the ethical standards of the Declaration of Helsinki.

2.2. Gene testing

After obtaining parental informed consent, peripheral blood samples were collected from the child and his parents to conduct trio-WES and gain further insights into the underlying causes of the child's disease. Genomic DNA was extracted from whole blood samples for library preparation using the Blood Genome Column Medium Extraction Kit (Kangweishiji, China). The xGen Exome Research Panel v1.0 (IDT, Iowa, USA) was used to enrich the protein-coding exome of a parent-offspring trio. The raw data was sequenced onNovaSeq6000 platforms (Illumina). Reads were mapped to the hg19reference genome using BWA MEM. Genetic variations were discovered using the Samtools and Pindel applications. Variants were then annotated with ANNOVAR software.

We prioritized rare variants with a minor allele frequency <0.005 in the Genome Aggregation Database (gnomAD) and Exome Aggregation Consortium (ExAC). We retained potentially pathogenic variants, including frameshift, nonsense, canonical splice site, initiation codon, in-frame, and missense variants. Variants were further filtered based on inheritance models such as *de novo*, homozygous, compound heterozygous, and X-linked. Additionally, we conducted focused analysis on variants clinically relevant to the patient's phenotype. Sanger sequencing was used to perform the validation analysis. Finally, the variations were annotated in accordance with the standards established by the American College of Medical Genetics (ACMG).

2.3. Cell culture and plasmid construction

293T cells obtained from the Shanghai Cell Bank were cultured in high-glucose DMEM (Gibco, USA) supplemented with 10 % fetal bovine serum. The cells were maintained in a CO_2 incubator at 37 °C under 5 % CO_2. Plasmid transfection was performed in a 6-well plate using Lipofectamine 2000 (Thermo Fisher Scientific, USA) once the cell density reached 60 %.

Plasmid construction was performed as follows. The pECMV-3 × FLAG-N vector was utilized to generate *MED27*-WT, following the instructions provided by the Phanta® Max Super-Fidelity DNA Polymerase kit (Vazyme, #P505). The amplification primers used were as follows: R: 5′-ggtttaaacgggccctctagaCTACTGCCGGCAGGTCA-3'; F: 5′-aaggatgacgatgacaagcttATGGCGGACGTGATAAATGTCA-3'. To create the *MED27*-MUT group, the Mut Express MultiS Fast Mutagenesis Kit V2 (Vazyme, #C215) guidelines were followed. The amplification primers for *MED27*-MUT were R: 5′-TCACGCTGGAGtGCAGCGCCTGGATGGCACTA-3'; F: 5′-GCTGCaCTCCAGCGTGAGCAGGGTGTTCGACT-3'. After sequencing verification, plasmid amplification and extraction were performed.

2.4. Western blot (WB) experiment

After transfection, both wild-type and mutant *MED27* cells were treated with protein lysis buffer (Beyotime, China) to extract proteins for WB analysis. Cell lysates were then subjected to SDS-PAGE electrophoresis, followed by transfer onto a PVDF membrane and blocking for 2 h in TBS with 0.05 % Tween-20 (Beyotime, China) and 5 % skim milk powder. Primary antibodies, including β-Actin (8H10D10) Mouse mAb (Cat#3700, dilution 1:1000, Cell Signaling Technology, USA) and DYKDDDDKTag(9A3) Mouse mAb (Cat#8146, 1:1000) were incubated on the membrane overnight at 4 °C. Subsequently, the membrane was incubated with the secondary antibody, in this case, Anti-mouse IgG, HRP-linked (Cat#7076, 1:5000, Cell Signaling Technology, USA). Protein bands were visualized using an appropriate detection method, and band analysis was performed using Image J v1.46 software (NIH, Bethesda, MD, USA). Data analysis and graph plotting were conducted using GraphPad Prism 8 (GraphPad Software Incorporation, San Diego, CA,

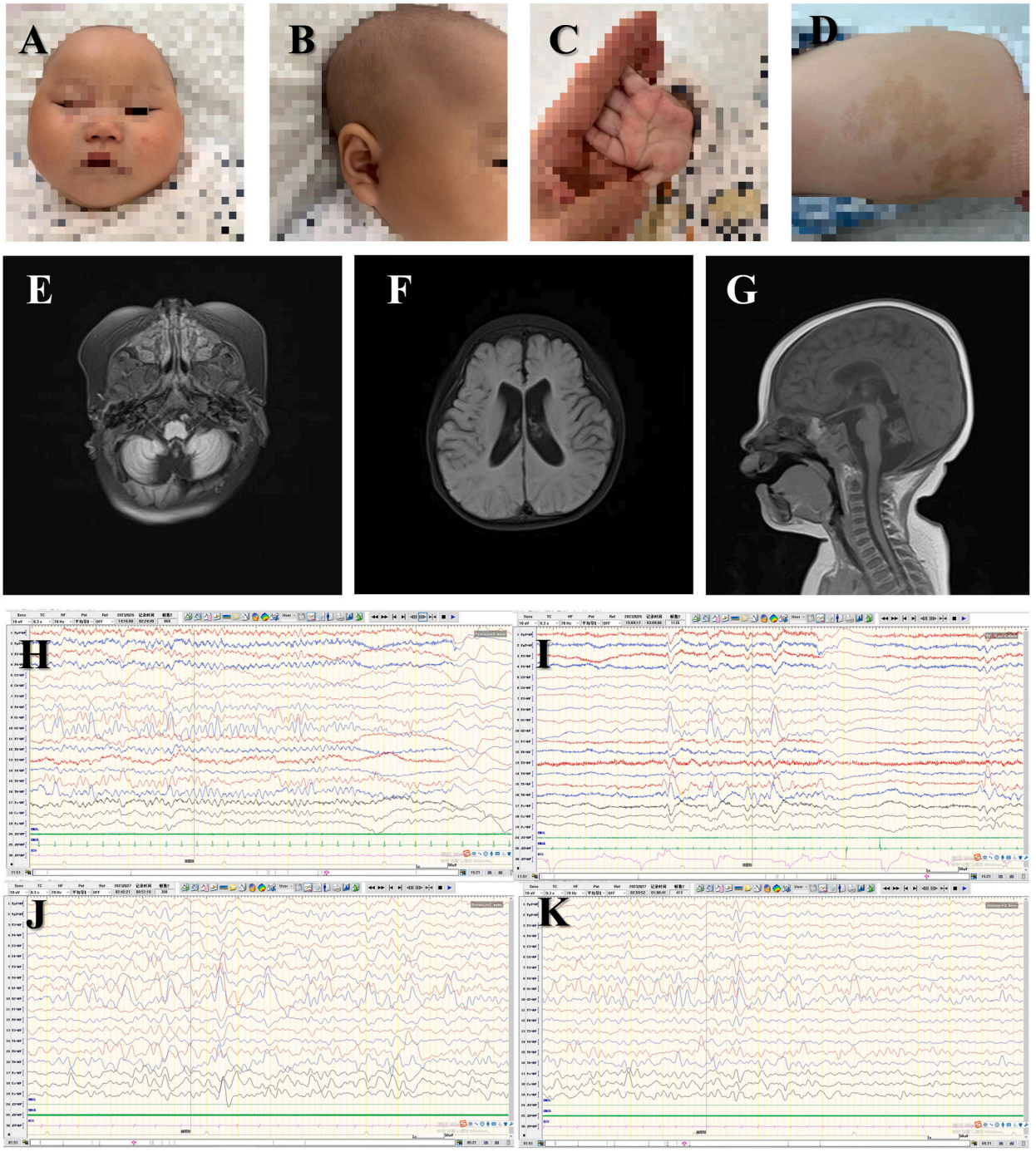

Fig. 1. A. Narrow forehead, upward-slanting corners of the eyes bilaterally and collapsed nose. B. Large ears. C. A hand through the palm. D. A large area of coffee-milk spot. MRI of the patient (6 months, E-G). E. T2-weighted imaging (T2WI): slightly smaller volume of bilateral cerebellar hemispheres. F. T2WI: slightly smaller volume of bilateral frontal lobes and slightly wider lateral ventricles. G. T1WI: a thinner body of corpus callosum and knees. Video Electroencephalograph (13 months, H-K). A large number of medium-high amplitude slow waves emanating, paroxysmal or continuous in the parietal, occipital, posterior temporal and midline regions in all phases of wakefulness and sleep, and non-synchronous in the left and right.

USA). Statistical significance was determined with three levels of significance ($p < 0.05$, $p < 0.01$, and $^{**}p < 0.001$). Each experiment was replicated three times.

2.5. Molecular dynamics simulation structure analysis

The RCSB PDB database (PDB: 7EMF, www.pdb.org/structure/7EMF) provided the structural data for the protein complex. The Modeller 10.1 database (https://salilab.org/modeller/) was employed to generate the protein's full-length tertiary structure as well as its three-dimensional structure. For the creation of the mutant structure, Pymol 2.5 (https://pymol.org/2/) was utilized. To study the behavior of both wild-type and mutant protein structures, a 10 ns molecular dynamics simulation was carried out using the GROMACS 5.1.4 computational package (http://www.gromacs.org/). The AMBER FF99SB force field was employed to optimize the properties of the structures. Afterwards, Chimera 1.15 (http://www.cgl.ucsf.edu/chimera/) was utilized to visualize the locally optimized structures and analyze their interactions.

3. Results

3.1. Case description

3.1.1. Clinical history

The male child was diagnosed with bilateral cataracts at the age of 2 months and subsequently underwent cataract surgery at 5 months of age. He presented with several physical characteristics, including a narrow forehead, upward-slanting corners of the eyes bilaterally, a flattened nasal bridge, an open mouth at rest, large ears, a palmar crease that extends across the hand, and a large coffee-milk spot (Fig. 1A–D). In terms of developmental milestones, the child demonstrated difficulties in holding his head up, rolling over, sitting steadily, and tracking with his eyes. His hearing development was also delayed. At the age of 7 months, he exhibited occasional teasing and laughter. Additionally, at 13 months of age, the child experienced a tonic-clonic seizure lasting approximately 1 min. Over four months, he had 2-3 episodes of similar seizures.

3.1.2. Auxiliary examination

The blood routine, biochemical, and endocrinologic examinations yielded normal results. The Video Electroencephalograph (VEEG) performed at 6 months of age showed normal findings. Cranial magnetic resonance imaging (MRI) performed at 6 months of age revealed a slight reduction in the volume of the bilateral cerebellar hemispheres, along with a widening of the corresponding occipital extracerebral space. Additionally, the volume of the bilateral frontal lobes was slightly decreased, the corpus callosum and knee showed thinning, and the white matter myelin development was comparable to that of a 1-month-old infant (Fig. 1E–G). Subsequent VEEG at 13 months of age demonstrated a sluggish background activity, with the presence of numerous slow waves originating from the midline area and posterior head during both wakefulness and sleep (Fig. 1H–K). The results of the Griffiths neurodevelopmental evaluation at 13 months indicated severe developmental delay, with a developmental level equivalent to approximately 1.5 months of age.

3.1.3. Diagnosis, treatment, and clinical follow-up

The patient's diagnosis of NEDSCAC was established based on the presence of a *MED27* variant as well as clinical manifestations characterized by congenital cataracts, developmental delay, and convulsive seizures. Following the explanation of the prognosis to the child's family, rehabilitation measures were initiated. However, the family opted not to administer anti-seizure medications (ASMs). Since the last presentation in September 2023, the child has not experienced any notable convulsive seizures. Furthermore, no substantial improvement or deterioration has been observed in their developmental progress.

3.2. Gene testing result

Based on the results of genetic testing, the child was found to have a homozygous missense variant (c.74G > A, p.(Arg25His)) in the *MED27* gene, which was inherited from non-consanguineous parents (Fig. 2A–C). The identified variants were corroborated through Sanger sequencing. Notably, this particular variant was absent in gnomAD v4.0.0 database (PM2_Supporting). The proband carries this variant in a homozygous state, and the clinical phenotype matches closely (PM3_Supporting). Therefore, c.74G > A, p.(Arg25His) variant can be classified as uncertain significance (VUS) (PM2_Supporting + PM3_Supporting) according to ACMG guidelines [9].

3.3. Protein expression analysis results

MED27 c.74G > A, p.(Arg25His) variant affected the N-terminal region of the MED27 subunit(Fig. 2D–E). To verify the pathogenicity of the gene locus, the expression of the MED27 protein was analyzed. Plasmid synthesis was performed for *in vitro* experiments, and WB analysis revealed the presence of expressed protein in both the MED27 Arg25His and MED27 Wild-type groups. However, it was observed that the MED27 Arg25His group exhibited a significant decrease in protein expression, approximately 77.42 %, compared to the MED27 Wild-type group (Fig. 2 F). However, the *in vitro* experience was only used to verify the expression level of the mutant protein, and it could not truly simulate the complex situation *in vivo*.

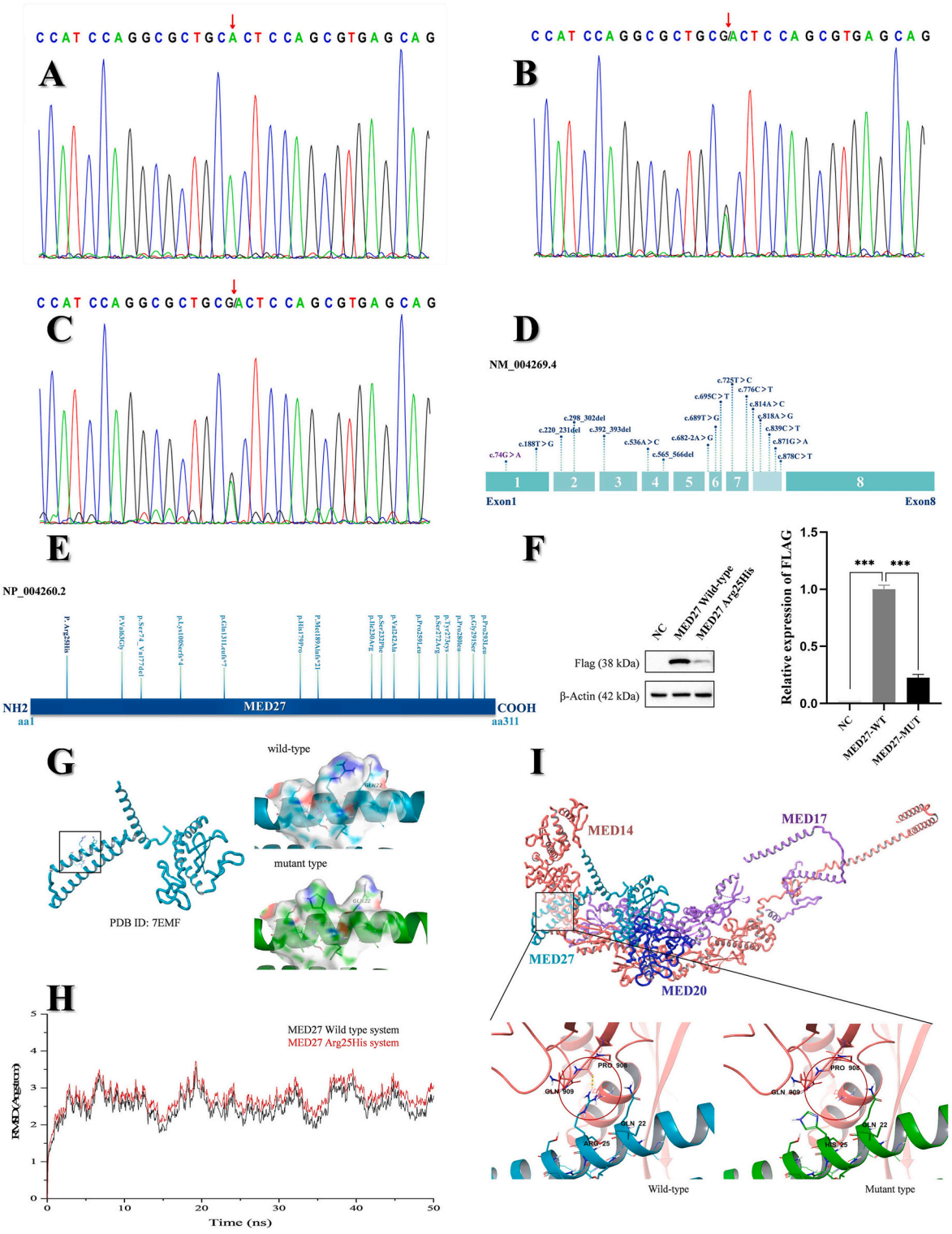

Fig. 2. Peak gene sequencing map(A-C). A. Proband. B. Father of the proband. C. Mother of the proband. Schematic diagram of *MED27* gene and protein (D–E). D. Blue font indicates the location of previously reported variants and purple font indicates the location of new variants. Introns are not to scale. Exon numbering in the canonical transcript (NM_021723.5). E. Amino acid variant c.74G > A of *MED27*, the Arg25His variant is closest to the N-terminus of the MED27 protein (indicated in dark font). Refer to amino acid variants in sequence NP_004260.2. F. The Western blot results revealed a significantly reduced expression of the MED27 Arg25His group compared to the MED27 Wild-type group, showing a decrease of approximately 77.42 % (***, $p < 0.001$). Protein structure analysis (G–I). G. Arg25 in MED27 protein (PDB ID: 7EMF) is located on the protein

surface (black box), although this variant did not show significant structural changes. However, reducing polarity may weaken the interaction with aqueous solvents, leading to a decrease in protein stability. H. The average Root mean square deviation (RMSD) values were calculated to balance the wild-type and mutant structures (MED27 complexed with MED20, MED17, and MED14 proteins), reaching equilibrium at 2.8 Å and 3.0 Å, respectively. I. In the complex system, the mutant MED27 protein (Arg25His) disrupts the hydrogen bonding interaction between MED27 and MED14 at Pro908 (red circle), which may lead to a reduced interaction force between MED27 and MED14 proteins.

3.4. Molecular dynamics simulation structure analysis result

The crystal structure of MED27 is currently incomplete, with unresolved regions at amino acids 79–103 and 140–155. Arg25 is located on the alpha helix of the protein surface. Although no changes were observed in the surrounding residues of the Arg25His variant, the presence of the imidazole propionic acid structure of histidine residues may introduce local steric hindrance. Simultaneously mutating may weaken the interaction with aqueous solvents, leading to a decrease in protein stability (Fig. 2 G). It is established that the MED27 protein forms a complex and carries out biological functions through interactions with MED20, MED17, and MED14 proteins [10]. By assessing the Root mean square deviation (RMSD) between the wild type and mutant complex systems, the average RMSD values were determined to be 2.8 Å and 3.0 Å, respectively (Fig. 2H). The findings indicated that the Arg25 variant in the mutant structure disrupted the hydrogen bonding interaction between MED27 Arg25 and MED14 Pro908 (Fig. 2 I). Furthermore, the analysis of binding energy suggested the mutant structure also resulted in higher van der Waals forces, with an approximately 12 % increase in the overall binding energy between MED27 and MED14 in the mutant structure, and thus a decrease in the stability of the mutant structure compared to the wild type (Table 1). In conclusion, the mutation of Arg25His of MED27 protein may lead to the weakening of the interaction with MED14 protein, which may reduce the structural stability of the whole protein system.

4. Discussion

NEDSCAC is an autosomal recessive disorder caused by variants in the *MED27* gene. Key features of this disorder include reduced white matter volume observed on brain MRI, cataracts, infantile hypotonia, and cerebellar atrophy [1,2]. *MED27*-related conditions manifest a spectrum of symptoms, ranging from dyskinetic encephalopathies to various neurodevelopmental disorders characterized by motor function impairments. Current research is limited to clinical phenotypes, genotypes, imaging findings, and their correlations. In this case, we present a child who exhibited congenital cataracts, developmental delay, convulsive seizures, as well as small cerebellar hemisphere volume and thin corpus callosum on cranial MRI. VEEG analysis detected a sluggish background activity with an abundance of slow waves originating from the midline area and the posterior head during both wakefulness and sleep. Genetic testing revealed a homozygous VUS missense variant in the *MED27* gene, specifically c.74G > A, p.(Arg25His). We performed *in vitro* functional experiments on the detected variants to further explore the pathogenesis.

The structure and subunit organization of the mediator complex exhibit conservation between yeast and humans. The MED complex comprises four modules: head, middle, tail, and CK8 kinase, with a composition of 25 subunits in yeast and 30 subunits in humans [10,11]. The MED tail is subdivided into two interconnected portions: a larger section (MED16, MED23, MED24, MED25) that links to the intermediate module via MED1's C-terminal region and MED14's C-terminus, and a smaller section (MED15, MED27, MED28, MED29, MED30) located adjacent to the head that wraps around MED14's C-terminal region [12,13]. The MED27 subunit is anchored to the core sequence by the C-terminal region of MED14, which also serves as a scaffold connecting the head, middle, and tail. Partial mass spectrometry analysis of the MED complex identified a limited number of high-confidence cross-links between MED27 and the C-terminus of MED14. MED27 consists of two distinct regions: an N-terminal region that forms a heterodimeric helical bundle with MED29, and a C-terminal globular structural domain that interacts with various head-segment proteins. Previous studies have shown that only one *MED27* variant (c.188T > G, p. (Val63Gly)) affected the N-terminal region of the MED27 subunit, which may have an effect on residues close to the MED29 interface [1,12]. All other *MED27* variants affected the C-terminus of the MED27 subunit. Whereas our study involved a case of the second current *MED27* c.74G > A, p.(Arg25His) variant that affected the N-terminal region of the MED27 subunit, *MED27* c.74G > A, p.(Arg25His) variant was closer to the N-terminus than *MED27* c.188T > G, p.(Val63Gly) variant. Furthermore, we conducted *in vitro* functional validation of the *MED27* c.74G > A, p.(Arg25His) variant to gain a deeper understanding of how alterations in the *MED27* gene can impact MEDs at a structural and functional level. Initially, we assessed the effect of the variant on protein expression. WB analysis indicated that the protein expression of the *MED27* Arg25His group was reduced by approximately 77.42 % compared to the *MED27* Wild-type group, suggesting a decrease in protein expression for the *MED27* c.74G > A, p.(Arg25His) variant. Subsequently, we investigated the variant's influence on molecular dynamics and found that Arg25 is situated on the protein's surface. Although no changes were found in the surrounding residues of the Arg25His variant, the

Table 1
Binding energy analysis data between MED27 and MED14 proteins.

Combining the contribution term of free energy.	MED27 Wild type - MED 14 energy value (kJ/mol).	MED27 Arg25His - MED14 energy value (kJ/mol).
△Evdw	−199.81 ± 1.53	−135.21 ± 1.98
△Eelec	−25.88 ± 0.66	−47.77 ± 0.55
△GGB	109.98 ± 1.01	88.09 ± 1.52
△GSurf	−26.38 ± 0.98	−30.02 ± 0.66
△Gbind	−142.09 ± 1.69	−124.91 ± 2.01

presence of the imidazole propionic acid structure of histidine residues may cause local steric hindrance. This could decrease the interaction with aqueous solvents, resulting in a decline in protein stability. The binding energy analysis revealed that the variation structure resulted in increased van der Waals forces, with an approximately 12 % increase in the overall binding energy between MED27 and MED14 in the variation structure. This could affect the structural stability of the whole protein system.

In 2021, Meng et al. published the first report of a neurodevelopmental disorder characterized by spasticity, cataracts, and cerebellar hypoplasia resulting from a variant in the *MED27* gene. The authors described a highly consistent phenotype across 16 patients from 11 NEDSCAC families. The majority of these patients exhibited varying degrees of mental retardation, developmental delays, central hypotonia, spasticity of the limbs, and dystonia. Some patients also presented with epilepsy and cataracts, although no specific facial features were observed, except for a few individuals with dysmorphic features [1]. In the most recent follow-up data, developmental delays in cognition, language, and movement were observed in varying degrees, along with infantile hypotonia and bilateral cataracts, with the majority of patients undergoing surgical treatment for the cataracts [2]. In 2023, Maroofian et al. reported on 57 additional NEDSCAC patients (18 previously reported and 39 unreported) from 30 families (12 previously reported and 18 unreported). They also identified previously unrecognized neurological signs, such as gait ataxia, hypersalivation, and hyperreflexia [2]. The case presented in this report aligns with previous reports in terms of facial features (small head, narrow forehead, collapsed nose, low-set ears, etc.), congenital cataracts in both eyes, severe global developmental delay, and convulsive seizures. However, phenotypes not previously reported, including a through-the-palm hand and a large café au lait milk spot, warrant further investigation to ascertain their specificity.

The *MED27* gene study conducted in 2021 initially identified eleven variant sites, including one classical shear site, three code-shift variant sites, and seven missense variant sites. All families included in the study exhibited patients with missense variants. In 2022, Reid KM et al. reported two siblings born to inbred parents who carried the *MED27* gene variant c.839C > T, p.(Pro280Leu), as well as a missense variant c.1186G > A, p.(Gly396Ser) in the *SLC6A7* gene and a missense variant c.985A > T, p.(Arg329*) in the *MPPE1* gene [14]. Among the reported missense variant loci, both the c.839C > T, p.(Pro280Leu) and c.871G > A, p.(Gly291Ser) missense variant loci recurred in multiple families (3 out of 11). The 2023 report identified four novel missense variant sites and one deletion variant. Seven homozygous pathogenic missense *MED27* variants were also identified. There is no evidence that the clinical phenotypes differ in severity between heterozygous and homozygous variants. No homozygous or compound heterozygous shifts, nonsense, or spliced variants were found, indicating that these variants may be lethal to developing embryos [2]. The most frequently recurring missense variant in this analysis was c.871G > A, p.(Gly291Ser), observed in 11 out of 30 families (11/30). Other recurring missense variants included c.725T > C, p.(Val242Ala), found in 5 families (5/30), and c.839C > T, p.(Pro280Leu), detected in 4 families (4/30). These findings are generally in line with earlier reports. The report further examined the clinical phenotype-genotype association in detail. Children with mutant types c.871G > A, p.(Gly291Ser), and c.776C > T, p.(Pro259Leu) tended to exhibit phenotypes ranging from mild to moderate. Conversely, children with the variant type c.536A > C, p.(His179Pro) displayed severe to very severe abnormalities. Those with variant types c.725T > C, p.(Val242Ala) and c.839C > T, p.(Pro280Leu) exhibited phenotypes ranging from moderate to severe, and severe to very severe [2]. We herein present the identification of a homozygous missense variant (c.74G > A, p.(Arg25His)) in the *MED27* gene in a child whose parents carried the heterozygous missense variant (c.74G > A, p.(Arg25His)) in the *MED27* gene. The mode of inheritance aligns with the disease pattern. This variant has yet to be documented in publicly accessible databases, thereby expanding the *MED27* gene variant map. Currently, no discernible correlation has been identified between the child's genotype and clinical phenotype.

According to the 2021 report, the majority of patients exhibited imaging findings indicative of cerebellar hypoplasia, primarily affecting the vermis region. A smaller proportion of patients also displayed imaging evidence suggestive of progressive atrophy in the basal ganglia, cerebral, and cerebellar regions, along with enlarged ventricles, thinning of the corpus callosum, and myelin sheath degeneration [1]. In the 2023 report, imaging was performed on 36 out of 57 (63.1 %) subjects, and all of these individuals displayed various degrees of cerebellar atrophy, with the vermis being the most commonly affected site, consistent with previous findings. Some subjects also exhibited reduced white matter volume and ventricular enlargement. Additionally, 33.3 % (12/36) of the subjects underwent follow-up imaging, which revealed progressive cerebellar atrophy in all cases. The majority of subjects exhibited an ongoing reduction in white matter volume and/or atrophy of the basal ganglia, characteristic features often observed in neurodegenerative diseases. In the clinical presentation-neuroimaging correlation analysis conducted in this study, a severe or greater severity clinical phenotype was found to be associated with decreased white matter volume and moderate-to-severe cerebellar atrophy. Individuals who were unable to walk independently had a frequent occurrence of moderate to severe cerebellar atrophy and a high T2 signal in the cortical folia of the cerebellum [2]. In our reported patient, the imaging findings included white matter myelin hypoplasia, thinning of the corpus callosum and geniculate, and slightly reduced volumes of both the bilateral cerebellar hemispheres and bilateral frontal lobes. Based on previous research findings, it was postulated that there might be a correlation between the child's current imaging presentation and the severity of their clinical phenotype. Continual monitoring and assessment of the child are necessary to observe any potential progression of cerebellar atrophy.

Upon reviewing the diagnosis and treatment process of this case, starting from the family's identification of the child's developmental delay to their interaction with the Department of Rehabilitation, as well as the indeterminate cause of the developmental delay, and concluding with the genetic test results indicating a missense variant in the *MED27* gene, and the identification of a suspected convulsive seizure through EEG analysis, along with the recommendation for rehabilitation training, we find that the overall diagnosis and treatment process adheres to the established protocol. Nevertheless, this process has prompted some contemplation. Clinical manifestations of *MED27*-related disorders demonstrate similarities to other MED single-gene variants, such as *MED13*-associated disorders, characterized by varying degrees of global developmental delay inherited in an autosomal dominant manner [15], as well as *MED17* and *MED23*-associated disorders, which are inherited in an autosomal recessive manner. In contrast to the latter, largely

defined by delayed intellectual development, sometimes accompanied by epilepsy, the former is primarily recognized by microcephaly, severe developmental delay, seizures, and substantial brain atrophy [16,17]. The advancement of high-throughput sequencing technology has facilitated the prompt and accurate diagnosis of *MED27*-related disorders, thereby mitigating the need for lengthy diagnostic processes. Previous cases involving multiple patients from the same family displaying *MED27* gene variants have shown that the prenatal and perinatal histories were generally unremarkable. This may be attributed to the limitations of ultrasound or MRI techniques, coupled with the insufficient characterization of clinical phenotypes during the fetal period. To address this, obstetric testing and genetic counseling should adopt a more proactive approach in families affected by monogenic genetic disorders. The decision of whether to conduct genetic testing on the fetus and parents significantly influences pregnancy-related choices. Furthermore, genetic counseling becomes more challenging for physicians when faced with genetic variants of undetermined significance, where the fetal phenotype partially aligns, but the evidentiary chain remains inadequate. Consequently, conducting imperative functional validation of the gene locus is crucial. Additionally, addressing the issue of genetic heterogeneity within genetic variants is a complex aspect of genetic counseling, warranting the establishment of more standardized methodologies and guidelines.

5. Conclusions

In this study, we identified a child with a novel homozygous VUS missense variant c.74G > A, p.(Arg25His) in the *MED27* gene and performed *in vitro* functional experiments on the *MED27* c.74G > A, p.(Arg25His) variant, broadening the range of variants associated with the *MED27* gene and further exploring the pathogenesis of NEDSCAC.

Ethics approval and participant statement

The patient's data and analysis for this study were gathered from The Third Affiliated Hospital of Zhengzhou University. The patients' parents were informed verbally when the consultation that the data will be used to summarize clinical experience and conduct scientific research. The paper conceals the patients' information and will no damage or injury to the subjects. Thus, for this study, only verbal informed agreement was acquired from the patients' parents. This study was approved by the Medical Ethics Committee of The Third Affiliated Hospital of Zhengzhou University (Reference: 2023-(Pre)202). The study was conducted in accordance with the Declaration of Helsinki.

Data availability statement

The data associated with this study have not yet been deposited into a publicly available repository because of ethical and privacy restrictions. The data presented in this article are not readily available, requests to access the data should be directed to the corresponding author.

Funding

This work was supported by the Open Research of Henan Key Laboratory of Child Brain Injury and Henan Pediatric Clinical Research Center (Reference: KFKT2021003) and Henan Provincial Science and Technology Tackling Project (Reference: 242102311058).

CRediT authorship contribution statement

Gongao Wu: Writing – review & editing, Writing – original draft, Data curation. **Ruofei Lian:** Writing – review & editing, Validation, Data curation. **Mengchun Li:** Data curation. **Liang Jin:** Data curation. **Tianming Jia:** Writing – review & editing. **Lijun Wang:** Data curation. **Ling Gan:** Data curation. **Shichao Zhao:** Data curation. **Ruirui Liang:** Data curation. **Yan Dong:** Writing – review & editing, Resources, Project administration, Funding acquisition, Conceptualization.

Declaration of competing interest

The authors declare that they have no known competing financial interests or personal relationships that could have appeared to influence the work reported in this paper.

Acknowledgements

We would like to express our sincere gratitude to the patients who graciously participated in this study.

References

[1] L. Meng, P. Isohanni, Y. Shao, B.H. Graham, S.E. Hickey, S. Brooks, A. Suomalainen, P. Joset, K. Steindl, A. Rauch, A. Hackenberg, F.A. High, A. Armstrong-Javors, N.E. Mencacci, P. Gonzalez-Latapi, W.A. Kamel, J.Y. Al-Hashel, B.I. Bustos, A.V. Hernandez, D. Krainc, S.J. Lubbe, H. Van Esch, C. De Luca, K. Ballon, C. Ravelli, L. Burglen, L. Qebibo, D.G. Calame, T. Mitani, D. Marafi, D. Pehlivan, N.W. Saadi, Y. Sahin, R. Maroofian, S. Efthymiou, H. Houlden, S. Maqbool,

F. Rahman, S. Gu, J.E. Posey, J.R. Lupski, J.V. Hunter, M.F. Wangler, C.J. Carroll, Y. Yang, MED27 variants cause developmental delay, dystonia, and cerebellar hypoplasia, Ann. Neurol. 89 (2021) 828–833, https://doi.org/10.1002/ana.26019.

[2] R. Maroofian, R. Kaiyrzhanov, E. Cali, M. Zamani, M.S. Zaki, M. Ferla, D. Tortora, S. Sadeghian, S.M. Saadi, U. Abdullah, E. Ghayoor Karimiani, S. Efthymiou, G. Yeşil, S. Alavi, A.M. Al Shamsi, H. Tajsharghi, M.S. Abdel-Hamid, N.W. Saadi, F. Al Mutairi, L. Alabdi, C. Beetz, Z. Ali, M.B. Toosi, S. Rudnik-Schöneborn, M. Babaei, P. Isohanni, J. Muhammad, K. Sheraz, M. Al Shalan, S.E. Hickey, D. Marom, E. Elhanan, M.A. Kurian, D. Marafi, A. Saberi, M. Hamid, R. Spaull, L. Meng, S. Lalani, S. Maqbool, F. Rahman, J. Seeger, T.B. Palculict, T. Lau, D. Murphy, N.E. Mencacci, K. Steindl, A. Begemann, A. Rauch, S. Akbas, A. A. Dilruba, V. Salpietro, H. Yousaf, S. Ben-Shachar, K. Ejeskär, A.I. Al Aqeel, F.A. High, A.E. Armstrong-Javors, S.M. Zahraei, T. Seifi, J. Zeighami, G. Shariati, A. Sedaghat, S.N. Asl, M. Shahrooei, G. Zifarelli, L. Burglen, C. Ravelli, J. Zschocke, U.A. Schatz, M. Ghavideldarestani, W.A. Kamel, H. Van Esch, A. Hackenberg, J.C. Taylor, L. Al-Gazali, P. Bauer, J.J. Gleeson, F.S. Alkuraya, J.R. Lupski, H. Galehdari, R. Azizimalamiri, W.K. Chung, S.M. Baig, H. Houlden, M. Severino, Biallelic MED27 variants lead to variable ponto-cerebello-lental degeneration with movement disorders, Brain (2023), https://doi.org/10.1093/brain/awad257.

[3] C. Jeronimo, F. Robert, The mediator complex: at the nexus of RNA polymerase II transcription, Trends Cell Biol. 27 (2017) 765–783, https://doi.org/10.1016/j.tcb.2017.07.001.

[4] J.W. Yin, G. Wang, The Mediator complex: a master coordinator of transcription and cell lineage development, Development 141 (2014) 977–987, https://doi.org/10.1242/dev.098392.

[5] C. Schiano, A. Casamassimi, M. Rienzo, F. de Nigris, L. Sommese, C. Napoli, Involvement of Mediator complex in malignancy, Biochim. Biophys. Acta 1845 (2014) 66–83, https://doi.org/10.1016/j.bbcan.2013.12.001.

[6] J.M. Grants, G.Y. Goh, S. Taubert, The Mediator complex of Caenorhabditis elegans: insights into the developmental and physiological roles of a conserved transcriptional coregulator, Nucleic Acids Res. 43 (2015) 2442–2453, https://doi.org/10.1093/nar/gkv037.

[7] A.D. Clark, M. Oldenbroek, T.G. Boyer, Mediator kinase module and human tumorigenesis, Crit. Rev. Biochem. Mol. Biol. 50 (2015) 393–426, https://doi.org/10.3109/10409238.2015.1064854.

[8] M. Buendía-Monreal, C.S. Gillmor, Mediator: a key regulator of plant development, Dev. Biol. 419 (2016) 7–18, https://doi.org/10.1016/j.ydbio.2016.06.009.

[9] S. Richards, N. Aziz, S. Bale, D. Bick, S. Das, J. Gastier-Foster, W.W. Grody, M. Hegde, E. Lyon, E. Spector, K. Voelkerding, H.L. Rehm, Standards and guidelines for the interpretation of sequence variants: a joint consensus recommendation of the American College of medical genetics and genomics and the association for molecular pathology, Genet. Med. 17 (2015) 405–424, https://doi.org/10.1038/gim.2015.30.

[10] S. Rengachari, S. Schilbach, T. Kaliyappan, J. Gouge, K. Zumer, J. Schwarz, H. Urlaub, C. Dienemann, A. Vannini, P. Cramer, Structural basis of SNAPc-dependent snRNA transcription initiation by RNA polymerase II, Nat. Struct. Mol. Biol. 29 (2022) 1159–1169, https://doi.org/10.1038/s41594-022-00857-w.

[11] K.L. Tsai, X. Yu, S. Gopalan, T.C. Chao, Y. Zhang, L. Florens, M.P. Washburn, K. Murakami, R.C. Conaway, J.W. Conaway, F.J. Asturias, Mediator structure and rearrangements required for holoenzyme formation, Nature 544 (2017) 196–201, https://doi.org/10.1038/nature21393.

[12] L. El Khattabi, H. Zhao, J. Kalchschmidt, N. Young, S. Jung, P. Van Blerkom, P. Kieffer-Kwon, K.R. Kieffer-Kwon, S. Park, X. Wang, J. Krebs, S. Tripathi, N. Sakabe, D.R. Sobreira, S.C. Huang, S.S.P. Rao, N. Pruett, D. Chauss, E. Sadler, A. Lopez, M.A. Nóbrega, E.L. Aiden, F.J. Asturias, R. Casellas, A pliable mediator acts as a functional rather than an architectural bridge between promoters and enhancers, Cell 178 (2019) 1145–1158.e1120, https://doi.org/10.1016/j.cell.2019.07.011.

[13] K.L. Tsai, C. Tomomori-Sato, S. Sato, R.C. Conaway, J.W. Conaway, F.J. Asturias, Subunit architecture and functional modular rearrangements of the transcriptional mediator complex, Cell 157 (2014) 1430–1444, https://doi.org/10.1016/j.cell.2014.05.015.

[14] K.M. Reid, R. Spaull, S. Salian, K. Barwick, E. Meyer, J. Zhen, H. Hirata, D. Sheipouri, H. Benkerroum, K.M. Gorman, A. Papandreou, M.A. Simpson, Y. Hirano, I. Farabella, M. Topf, D. Grozeva, K. Carss, M. Smith, H. Pall, P. Lunt, S. De Gressi, E.J. Kamsteeg, T.B. Haack, L. Carr, R. Guerreiro, J. Bras, E.R. Maher, R. H. Scott, R.J. Vandenberg, F.L. Raymond, W.K. Chong, S. Sudhakar, K. Mankad, M.E. Reith, P.M. Campeau, R.J. Harvey, M.A. Kurian, MED27, SLC6A7, and MPPE1 variants in a complex neurodevelopmental disorder with severe dystonia, Mov. Disord. 37 (2022) 2139–2146, https://doi.org/10.1002/mds.29147.

[15] L. Snijders Blok, S.M. Hiatt, K.M. Bowling, J.W. Prokop, K.L. Engel, J.N. Cochran, E.M. Bebin, E.K. Bijlsma, C.A.L. Ruivenkamp, P. Terhal, M.E.H. Simon, R. Smith, J.A. Hurst, H. McLaughlin, R. Person, A. Crunk, M.F. Wangler, H. Streff, J.D. Symonds, S.M. Zuberi, K.S. Elliott, V.R. Sanders, A. Masunga, R.J. Hopkin, H.A. Dubbs, X.R. Ortiz-Gonzalez, R. Pfundt, H.G. Brunner, S.E. Fisher, T. Kleefstra, G.M. Cooper, De novo mutations in MED13, a component of the Mediator complex, are associated with a novel neurodevelopmental disorder, Hum. Genet. 137 (2018) 375–388, https://doi.org/10.1007/s00439-018-1887-y.

[16] R. Kaufmann, R. Straussberg, H. Mandel, A. Fattal-Valevski, B. Ben-Zeev, A. Naamati, A. Shaag, S. Zenvirt, O. Konen, A. Mimouni-Bloch, W.B. Dobyns, S. Edvardson, O. Pines, O. Elpeleg, Infantile cerebral and cerebellar atrophy is associated with a mutation in the MED17 subunit of the transcription preinitiation mediator complex, Am. J. Hum. Genet. 87 (2010) 667–670, https://doi.org/10.1016/j.ajhg.2010.09.016.

[17] A. Trehan, J.M. Brady, V. Maduro, W.P. Bone, Y. Huang, G.A. Golas, M.S. Kane, P.R. Lee, A. Thurm, A.L. Gropman, S.M. Paul, G. Vezina, T.C. Markello, W. A. Gahl, C.F. Boerkoel, C.J. Tifft, MED23-associated intellectual disability in a non-consanguineous family, Am. J. Med. Genet. 167 (2015) 1374–1380, https://doi.org/10.1002/ajmg.a.37047.